IMPACT MELTING, EXCAVATION, AND REDEPOSITION OF CRUSTAL COMPONENTS WITHIN THE ARTEMIS EXPLORATION ZONE: IMPLICATIONS FOR EVA SAMPLING. David A. Kring[1], [1]Center for Lunar Science and Exploration, Lunar and Planetary Institute, Universities Space Research Association, 3600 Bay Area Blvd., Houston, TX 77058 (kring@lpi.usra.edu).

Introduction: The Artemis exploration zone is an impact-cratered terrain. To adequately prepare for one or more geological expeditions to the region, it is necessary to evaluate the impact events that shaped that terrain. It is also important to evaluate the distribution of lithologies that might be collected and the information they may contain about the 'big ideas' of lunar science [1].

Margin of the SPA Basin: The Artemis exploration zone straddles the margin of the South Pole-Aitken (SPA) basin, which was detected in telescopic images as a semi-circular ring of Leibnitz Mountains along the south polar limb of the Moon [2]. Two potential rings of massifs were mapped following the Clementine mission [3]. One of those massifs, 1,900 m-high, was partially excavated by the ~3.43 Ga [4] Shackleton impact event. A portion of the massif appears to be composed of pure anorthosite [5,6].

Shackleton Ejecta: Shackleton ejecta covers the remaining portion of the massif. Hydrocode simulations of the impact [7] suggest the ejecta is ~150 m thick on the crater rim and thins with distance over the massif towards Henson crater. The mass of the largest block (m_b) in ejecta is proportional to the total ejected mass (M_e), $m_b \propto M_e^{0.8}$ (e.g., [8]), implying the mass of the largest block around Shackleton crater may be ~10^{13} g. Assuming an anorthosite density of 2.6 g/cm^2 (i.e., previously damaged by shock during bombardment in the first billion years of lunar history), the largest block may be ~150 m, close to the largest rock exposures observed in Shackleton ejecta [6]. Rock exposures of that size were not available at Apollo sites, so if that material can be examined during an EVA, it would provide a unique opportunity to observe intrusive and/or crystallization textures that provide clues about the magmatic system(s) that generated lunar anorthosite.

Assessing the Lunar Magma Ocean Hypothesis & Evolution of the Lunar Crust: The crust in the Artemis exploration zone was notionally produced from a lunar magma ocean [9] and covered by SPA ejecta. The crust may have been crudely stratified, with a relatively mafic norite and anorthositic norite base, a middle anorthosite layer, and a mixed anorthositic norite or noritic anorthorsite layer on top [10]. Elsewhere on the Moon, a pure anorthosite layer may occur between 30 and 63 km depths [11]. Thus, the observation of pure anorthosite at the surface in the Shackleton massif is an intriguing anomaly.

The Artemis exploration zone was modified by several impact cratering events between the formation of SPA (circa 4.35 Ga) and Shackleton; e.g., Henson, Haworth, Shoemaker, Faustini, de Gerlache, Nobile, Slater, Scott, Sverdrup, Cabeus, Amundsen, and Schrödinger. Those impact events excavated and melted material from depth and deposited that material on the surface. Using the crater diameters of [12] and a simple scaling relationship (e.g., [13]), depths of excavation range from 1.8 (for Shackleton) to 27 km (for Schrödinger). Our computer simulation of the Schrödinger impact [14] suggests shallower depths of excavation of 19 to 24 km. Using our solution for impacts into anorthositic crust [15], melt volumes can also be calculated (**Fig. 1**). If we assume those melt volumes are spherical, then depths of melting range from 2.1 km (Shackleton), to 5.8 km (Haworth, Shoemaker), 12 km (Cabeus, Amundsen), and 44 km (Schrödinger). Those depths will be upper limits, because melted volumes are actually paraboloids rather than spheres (e.g., [16] and Fig. 1 of [17]). For example, our computer simulations of the Shackleton [7] and Schrödinger [14] impacts indicate melting depths of ~1.6 km and 25 to 30 km, respectively. Thus, crater excavation and melting would have been limited to the upper 30 km among those craters having the greatest effect on the Artemis exploration zone.

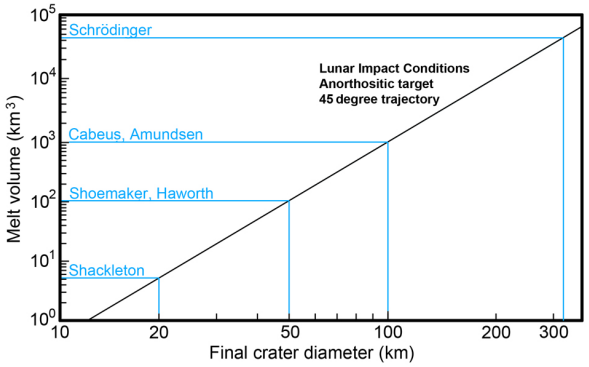

Fig. 1. Approximate impact melt volume for representative craters affecting the Artemis exploration zone.

Orbitally-determined compositions of the Artemis exploration zone soil suggest that the impact-distributed material is relatively homogeneous with ~80 to 90 wt% plagioclase and ~5 to 10 wt% FeO, mostly in the form of low-Ca pyroxene, but with some high-Ca pyroxene and olivine [18]. Those data are consistent with a noritic

anorthosite, but not a gabbroic anorthosite or anorthositic norite upper crustal layer. In the Artemis III candidate landing region 'Connecting Ridge,' where Shackleton ejecta covers the surface, exposures of pure anorthosite occur [18]. Artemis III candidate landing regions 'Nobile Rim 1' and 'Leibnitz Beta Plateau' may have the least plagioclase [18].

SPA Ejecta: Lunar magma ocean products are notionally covered with SPA ejecta [10]. That event produced nearly half the impact melt during the basin-forming epoch (**Fig. 2**; [19]). Our modeling suggests ~20% [20] of the impact melt was ejected from the central transient crater and cooled without significant differentiation [21]. Our model calculations [22] also suggest quenched SPA impact melt in the outer portions of the SPA basin would have had a moderately enriched FeO content (~15 wt% FeO). That said, it is possible (as in the case of the Chicxulub impact event on Earth) that ejected melts [23] do not reflect well-mixed average crustal compositions [24], but instead reflect a range of target rock compositions [25,26] with a disproportional component from shallower target materials.

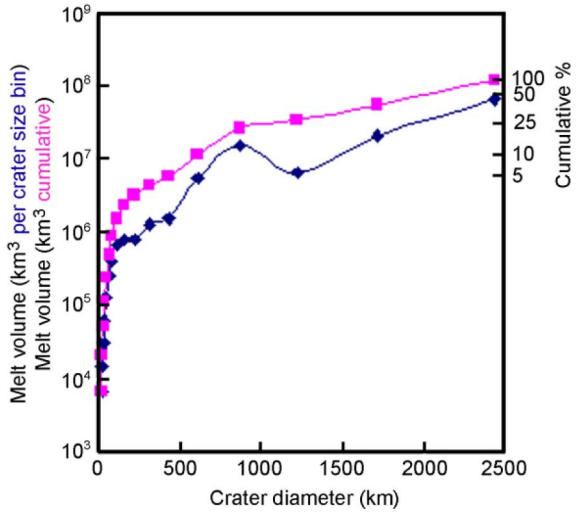

Fig. 2. Impact melt volumes for ancient lunar highland crater populations in crater size bins ranging from 8 to 2,500 km.

Unspecified enrichments of mafic material in the Artemis exploration zone may be ejecta from SPA [27]. Yet, it is important to remember that pristine anorthosite in the Apollo collection has a wide range (8.1 ± 8.6 wt% [28]) of mafic components. We note, too, that Imbrium and Orientale ejecta were added to the region, possibly with mafic compositions like those at Apollo sites. Thus, to interpret orbital assessments of mafic components correctly, it will be important during EVAs to collect anorthosite samples like that seen near Shackleton [6,7] and impact breccias at any Artemis landing site that will contain an assortment of clasts that reveal the diversity of anorthositic and mafic materials in the region.

Assessing the Lunar Cataclysm Hypothesis: Impact lithologies suitable for geochronology will be universal to the Artemis III candidate landing regions. Within the 'Connecting Ridge' region, the primary accessible geologic samples during EVA will be Shackleton ejecta, potentially including Shackleton impact melts, from which the 3.43 Ga model age can be tested. Elsewhere throughout the region, samples of SPA ejecta may occur, which will allow the age of the oldest basin to be determined. Each of the candidate regions will provide additional opportunities to test other model ages [29,12], albeit not necessarily all of them at the same location.

Summary: EVA sampling at Artemis III candidate landing regions will allow tests of several crustal concepts: (1) massif formation, (2) anorthosite formation, (3) the lunar magma ocean hypothesis, and (4) the lunar cataclysm hypothesis. Because the Shackleton impact event appears to have excavated pure anorthosite, the Artemis III candidate landing site 'Connecting Ridge' may be unique among the thirteen sites being considered.

References: [1] Kring D. A. (2020) *Lunar Surface Science Workshop*, Abstract #5037. [2] Hartmann W. K. and Kuiper G. P. (1962) *Comm. LPL*, No. 12, 51–66 & 77 plates. [3] Spudis P. D. et al. (2008) *GRL, 35,* 5 p., L14201. [4] Kring D. A. et al. (2021) *Adv. Space Res., 68,* 4691–4701. [5] Yamamoto S. et al. (2012) *GRL, 39,* L13201. [6] Gawronska A. J. et al. (2020) *Adv. Space Res., 66,* 1247–1264. [7] Halim S. H. et al. (2021) Icarus, 354, 113992, 9p. [8] Gault D. et al. (1963) NASA TN-D-1767. [9] Wood J. A. et al. (1970) *Science, 167,* 602–604. [10] Hawke B. R. et al. (2003) *JGR, 108,* E6, 5050. [11] Donaldson Hanna K. L. et al. (2014) *JGR, 119,* 1516–1545. [12] Deutsch A. N. et al. (2020) *Icarus, 336,* 113455, 10p. [13] Flahaut J. et al. (2012) *Adv. Space Res., 50,* 1647–1665. [14] Kring D. A. et al. (2016) *Nature Comm., 7,* 10 p., 13161. [15] Abramov O. et al. (2012) *Icarus, 218,* 906–916. [16] Kring D. A. (1995) *JGR, 100,* 16979–16986. [17] Kring D. A. and Durda D. D. (2002) *JGR, 107,* E8, 5062. [18] Lemelin M. et al. (2022) *Planet. Sci. J., 3*:63, 14p. [19] Kring D. A. et al. (2012) *LPS XLIII,* Abstract #1615. [20] Potter R. W. K. et al. (2012) *Icarus, 220,* 730–743. [21] Hurwitz D. and Kring D.A. (2015) *EPSL, 427,* 31–36. [22] Hurwitz D. and Kring D. A. (2014) *JGR, 119,* 1110–1133. [23] Kring D. A. and Boynton W. V. (1991) *Geochim. Cosmochim. Acta, 55,* 1737–1742. [24] Kring D. A. (1997) *LPS XXVIII,* Abstract #1084. [25] Izett G. (1991) *JGR, 96,* 20,879–20,905. [26] Sigurdsson H. et al. (1991) *Nature, 349,* 482–487. [27] Moriarty D. P. III and Petro N. E. (2020) *LPS LI*, Abstract #2428. [28] Warren P. H. (1990) *Am. Mineral., 75,* 46–58. [29] Tye A. R. et al. (2015) *Icarus, 255,* 70–77.